Low-Temperature Water-Gas Shift: In-Situ DRIFTS−Reaction Study of a Pt/CeO_2 Catalyst for Fuel Cell Reformer Applications

Gary Jacobs, Leann Williams, Uschi Graham, Dennis Sparks, and Burtron H. Davis*

Center for Applied Energy Research, University of Kentucky, 2540 Research Park Drive, Lexington, Kentucky 40511

Received: February 12, 2003; In Final Form: July 22, 2003

Steady-state IR measurements for adsorption of only CO and under WGS reaction indicate that formates are present on the surface of partially reduced ceria, in contrast to a recent study, and that they are strongly limited at high CO conversions. At low temperatures and conversions, the formates are close to the equilibrium adsorption/desorption coverages obtained from CO adsorption alone. The formates are close to saturation at low temperatures. These IR results favor the bidentate formate mechanism in explaining WGS. However, more kinetic studies are required and over a wider range of temperatures. While low-temperature kinetic studies have found a zero-order dependency for CO and related this to saturation of a noble metal surface, this study indicates that one cannot rule out the possibility of the formate mechanism on this basis, as CO is also close to saturation as an adsorbed formate at the low temperatures used in previous studies.

1. Introduction

Fuel-cell technology is currently undergoing rapid development for both stationary and transportation applications. As a low emission, energy-efficient process, it is possible that fuel cells may replace the internal combustion engine for automotive applications. Recent developments indicate that water-gas shift (WGS) catalysts may be important for the low-temperature production of hydrogen for polymer−electrolyte fuel cells (PEFC), also referred to as proton-exchange-membrane fuel cells (PEMFC).

One attractive option for achieving fuel flexibility for the production of H_2 involves steam reforming and partial oxidation of hydrocarbons. The resulting products from these reactions will contain CO, CO_2, H_2O, and CH_4. CO is especially problematic, because even levels on the order of 10 ppm poison platinum catalysts for anodes under normal fuel cell conditions.[1,2] Moreover, CO is a criterion pollutant.

Converting CO from the hydrogen-rich formate stream is typically conducted in stages. If hydrocarbons are reformed, a typical product stream containing 8−10% CO first is processed by high-temperature WGS (HTS) at close to equilibrium to reduce levels to 3−5% CO. Medium-temperature shift (MTS) and low-temperature shift (LTS) are used to convert CO to <1%, which can be handled by a preferential oxidation (PROX) cleanup system.[3] Since LTS is limited by kinetics, this is where the current demand for advanced catalysts is the greatest.

Metal-promoted ceria catalysts are currently being studied by a number of groups as potential candidates which may, with proper development, exceed the activities of today's commercial Cu−ZnO catalysts.

The overall reaction is as follows:

$$CO + H_2O \rightarrow CO_2 + H_2,$$
whereby $\Delta H = -41.2$ kJ/mol, and $\Delta G = -28.6$kJ/mol

The use of highly active LTS catalysts, in conjunction with effective PROX catalysts, may allow developers to avoid the implementation of costly hydrogen-permeable membranes.

There has recently been interest in new low-temperature WGS catalysts for hydrogen production. However, an effective commercial catalyst has remained elusive. One catalyst receiving widespread attention as a good low-temperature WGS catalyst is ceria loaded with promoter metals, such as platinum, rhodium, palladium, nickel, iron, and cobalt.

However, there is still disagreement as to the role of ceria in the WGS reaction mechanism. Primarily, there are two schools of thought for metal-promoted ceria catalysts. One recently proposed mechanism involves a ceria-mediated redox process, whereby CO adsorbed on the metal is oxidized by ceria. The second step in the concerted mechanism involves reoxidation of the ceria by water. It was proposed by Bunluesin et al.[4] that, in this redox mechanism, oxygen transfer from ceria to the metal interface, as well as the reoxidation step, together control the WGS reaction rate. The basis for this mechanism was supported by kinetic testing,[5] where it was found that the rate dependence of CO was zero-order. The zero-order dependency was expected on the basis of their proposed mechanism, as the noble metal surface was found to be saturated with CO under the low reaction temperatures studied and relatively high CO/H_2O ratio employed.

However, an earlier explanation for noble metal-promoted ceria catalysts proposed by Shido and Iwasawa[6,7] is that bidentate formate, produced from CO, and terminal ceria surface OH groups on partially reduced ceria, could act as an intermediate. In that scheme, the bidentate formate is decomposed to hydrogen and unidentate carbonate, prior to the liberation of CO_2. It is known that formates form on partially reduced ceria by adsorption of CO.[8]

In this work, DRIFTS has been utilized as a technique in studying noble metal-promoted WGS catalysts. The following study examines species evolved after adsorption of CO alone onto reduced Pt/ceria catalysts, and their response under steady-state WGS reaction in order to gain further insight into the mechanism. Special attention is paid to the use of N_2 as a

* Corresponding author. Phone: (859) 257-0251. Fax: (859) 257-0302.

10.1021/jp0302055 CCC: $25.00
Published on Web 08/28/2003

TABLE 1: Results of Catalyst Pulse Reoxidation Measurements (300 °C)

description	BET SA (m^2/g)	O_2 cons. ($\mu mol/g_{cat}$)
0.6% Pt/ceria (cerium nitrate decomposition)	55	92
1% Pt/ceria (urea)	100	197

balancing gas to fix the partial pressure of CO constant under adsorption of CO alone, and after the N_2 is replaced by H_2O to run the reaction at steady state in the cell.

However, instead of using a high CO/H_2O ratio, where the rate exhibits a zero-order dependency on CO and the adsorbed CO surface intermediate should remain close to saturation under WGS, we chose a high H_2O/CO ratio of partial pressure, where the rate is first-order in CO, and the adsorbed CO intermediate must move to sparser coverages with the WGS rate. Indeed, these kinetics are well-known for metal−ceria systems,[9] and could describe either mechanism, as follows:

$$\text{rate} = \frac{k_1 k_2 P_{CO} P_{H_2O}}{k_1 P_{CO} + k_2 P_{H_2O}}$$

2. Experimental Section

2.1. Catalyst Preparation. Ceria was prepared by decomposition of cerium nitrate through calcination under air flow at 500 °C. The platinum was loaded by incipient wetness impregnation (IWI) of the ceria using tetraammineplatinum(II) nitrate. The loading of Pt was verified by inductively coupled argon plasma (ICP) to be 0.6 wt %. Two other catalysts were prepared with higher Pt loadings of 1 and 2 wt %. The surface areas of the ceria and 0.6% Pt/ceria catalyst were measured by nitrogen adsorption using a Micromeritics Tri-Star system, and both were found to be 55 m^2/g.

A higher-surface-area ceria support was prepared by the urea coprecipitation−gelation method.[9] On a 30 g basis, an appropriate amount of $Ce(NO_3)_3 \cdot 6H_2O$ (Alfa Aesar, 99.5%) and 240 g of urea were dissolved in 900 mL of deionized water, and to the solution NH_4OH (Alfa Aesar, 28−30% NH_3) was added dropwise (1 mL/min.). The mixture was boiled at 100 °C with constant stirring. The precipitate was filtered, washed with 600 mL of deionized water, and dried at 100 °C. The ceria was crushed and calcined in a muffle furnace for 4 h. An amount of 1% Pt by weight was loaded by IWI, and the catalyst was recalcined. The BET surface area of the ceria was found to be 105 m^2/g, while the Pt-containing catalyst was 100 m^2/g (see Table 1).

2.2.Temperature-Programmed Reduction (TPR). TPR was conducted on both the Pt/CeO_2 catalyst and the unpromoted CeO_2 in a Zeton-Altamira AMI-100 unit equipped with a thermal conductivity detector (TCD). Argon was used as the reference gas, and 10% H_2, balance argon, was flowed at 30 cm^3/min as the temperature was increased from 50 °C to 800 °C at a ramp rate of 10 °C/min.

2.3. Pulse Reoxidation. Degree of reduction measurements were conducted following catalyst reduction in hydrogen using the Zeton-Altamira AMI-200 unit. The sample amount was 0.220 g. Catalysts were reduced at 300 °C for 2 h. The hydrogen was purged with a flow of helium prior to adding pulses of oxygen from a sample loop. Saturation was achieved when the entire O_2 pulse was observed by the TCD. After reoxidation, the number of moles of O_2 uptake was determined.

2.4. Diffuse Reflectance Infrared Fourier Transform Spectroscopy and Reaction Testing. A Nicolet Nexus 870 was used, equipped with a DTGS-TEC detector. A high-pressure/high-temperature chamber fitted with ZnSe windows was utilized as the water-gas shift reactor for in-situ reaction measurements. The gas lines leading to and from the reactor were heat traced, insulated with ceramic fiber tape, and further covered with general purpose insulating wrap. Scans were taken at a resolution of 4 to give a data spacing of 1.928 cm^{-1}. Typically, 128 scans were taken to improve the signal-to-noise ratio, but in some cases, as few as 2 scans were taken to observe transient responses when switching among desired gases. The sample amount was always 30 mg.

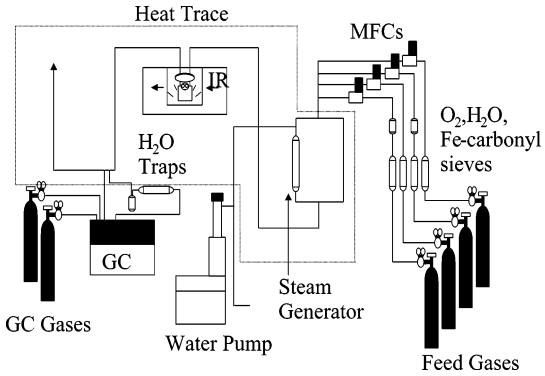

Figure 1. Schematic of the in-situ DRIFTS-rxn system.

A steam generator consisted of a downflow tube packed with quartz beads supported on quartz wool and equipped with an internal thermocouple. The tube was heat traced and run at the same temperature as that maintained at the in-situ sample holder. This allowed us to accurately bring the reactants to the desired reaction temperature. Water was added to the steam generator by a thin needle that was attached to a 1/16th inch (0.16 cm) line. A precision ISCO model 500D syringe pump was used to feed the water.

A gas chromatograph (SRI 8610C) was used to monitor the reaction products. The GC includes two columns (packed 1.8 m silica gel and packed 0.9 m molecular sieve) and two detectors (FID and TCD). To improve the sensitivity of the CO and CO_2 signals, the GC incorporates a methanizer, so that these products can be analyzed by FID. An internal standard of N_2 flow allowed for more accurate assessment of the CO conversion, on the basis of the CO/N_2 ratio. A bypass line allowed the flow to be directed to a 40 cm^3 knockout trap containing Drierite, followed by a Supelco water-absorbing molecular sieve, prior to sending the dry gas to the purge valve of the GC.

The outlet to the DRIFTS cell was equipped with a back pressure valve set at 0.027 MPa. This resistance helped to stabilize the system from pressure swings due to filling of the water knockout trap, during sampling through the bypass. Several GC samples were taken to ensure that the traps had been cycled with enough product gas to obtain a representative sample. Only the CO and N_2 were analyzed by FID and TCD, respectively.

Feed gases were controlled by using Brooks 5850 series E mass flow controllers. Iron carbonyl traps consisting of lead oxide on alumina (Calsicat) were placed on the CO_2 and CO gas lines. All gas lines were filtered with Supelco H_2O/moisture traps. The CO_2 regulator was equipped with a heater to prevent condensation through the restriction. A schematic of the system is displayed in Figure 1.

Results and Discussion

3.1. Catalyst Reduction. To reduce the catalyst, a H_2/N_2 mixture (100:135 cm^3/min) was introduced after purging in N_2

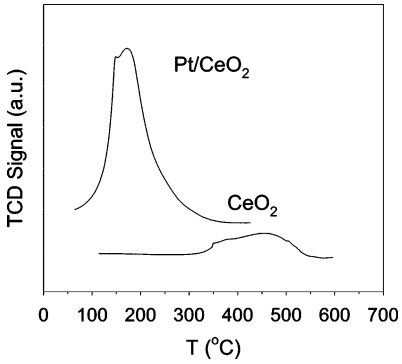

Figure 2. TPR profiles for the reduction of unpromoted and 0.6% Pt/ceria.

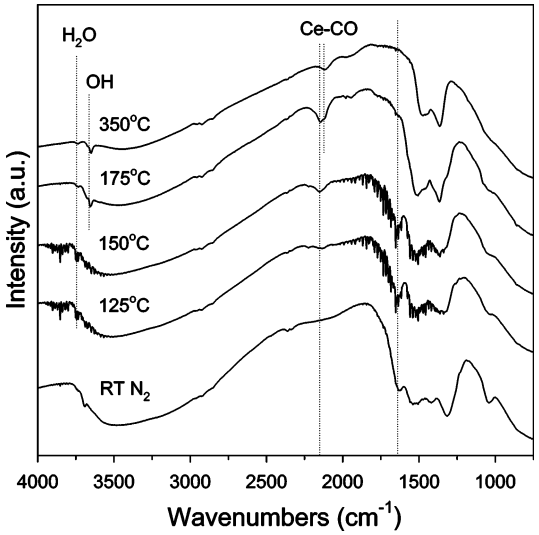

Figure 3. In-situ DRIFTS spectra of the reduction of the Pt/CeO_2 catalyst.

at room temperature. Scans were taken every 25 °C. At approximately 125 °C, displayed in Figures 2 and 3, reduction of the Pt occurred, as well as reduction of the CeO_2 surface in contact with the metal. Therefore, Pt appears to aid in reducing the ceria via spillover from the reduced metal. Interestingly, we observed the removal of a band located at 1630 cm^{-1}. As the band disappeared, a band formed at 2150 cm^{-1}, likely corresponding to Ce−CO,[10] where CO is adsorbed on Ce^{4+}. As there are not any C−H stretching bands accompanying the 1630 cm^{-1} band, we tentatively assign the disappearing band to a possible surface carbonate. At 175 °C, we observed two bands, one situated at 2150 and another at 2120 cm^{-1}, consistent with the assignment of Ce−CO,[10] where CO is adsorbed on Ce^{3+}. The band at 2150 cm^{-1} disappeared with increasing temperature and overnight reduction in H_2 at 350 °C, but a small band at 2120 cm^{-1} remained.

Interesting changes were also noticed in the OH stretch region (>3500 cm^{-1}). At temperatures lower than the reduction temperature, an OH band is situated at 3700 cm^{-1}. However, at the reduction temperature, when water was formed, gas-phase water appears at 3745 cm^{-1}. The rotational spectra are clearly visible. After reduction, the band at 3745 cm^{-1} decreases in intensity and shifts to 3740 cm^{-1}, and bands at 3650 and 3675 cm^{-1} (shoulder) are formed, corresponding to ceria surface geminal OH groups.[6,7,10]

Considering the assignments summarized by Holmgren et al.,[10] the bands at 3650 cm^{-1} (with 3675 cm^{-1} shoulder)

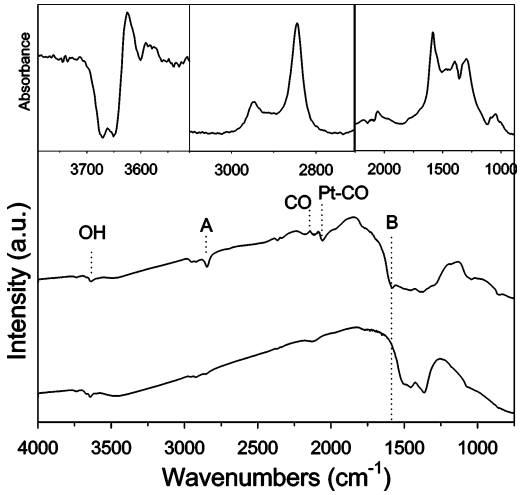

Figure 4. Adsorption of CO at 350 °C. The single-beam spectrum of the reduced catalyst, purged in N_2, is displayed at the bottom, while the spectrum after adsorption of CO, is shown above. Difference spectra are indicated above in absorbance units. Species A likely corresponds to C−H stretch of formate, while species B is the corresponding asymmetric OCO.

correspond to geminal OH groups on Ce and 3710 cm^{-1} to unidentate Ce−OH, and conclusions can be tentatively made. During reduction, the Pt metal is reduced and catalyzes partial reduction of the ceria surface, presumably by spillover from the reduced metal. Apparently, surface cerium carbonate present after the calcination procedure decomposed and CO was liberated from Ce^{4+} and Ce^{3+}, as bands for Ce−CO are readily apparent for both assignments, along with a band for Pt−CO. Reduction of the Pt oxide with hydrogen, as well as reduction of ceria through reaction with adsorbed Pt−H results in the liberation of water (band appears at 3745 cm^{-1}), and $Ce-(OH)_2$ geminal groups emerge in the spectra after reduction, consistent with the findings of Shido and Iwasawa.[6,7]

To further quantify the extent of reduction of surface ceria, O_2 uptake measurements were carried out after reduction in hydrogen at 300 °C. The high-surface-area catalyst gave much higher uptakes of O_2 (Table 1). Note that the uptake measurements do not reflect bulk reduction of ceria, which occurs above 700 °C.[9,11,12]

3.2. Reaction Studies. In the first reaction testing experiment, the catalyst, reduced at 350 °C under hydrogen, was purged in N_2, followed by addition of CO (3.75 cm^3/min) in N_2 (135 cm^3/min) at 350 °C. The single-beam spectra, and the corresponding difference spectra, in absorbance, are shown in Figure 4. After adsorption of CO, bands appear in the so-called "carbonate" region at 1045, 1085, 1295, 1330 (shoulder), 1390, 1475, 1560 (shoulder), and 1585 cm^{-1}, respectively. The strongest bands appear at 1585 (indicated by "B") and 1390 cm^{-1}, likely corresponding to formates, while there are also present weaker bands at 1560, 1295, and 1045 cm^{-1} corresponding well to the assignments of bidentate carbonates summarized by Holmgren et al.[10] The peak at 2060 cm^{-1} indicates CO adsorbed linearly on highly dispersed Pt. The gas-phase CO appears from 2000 to 2150 cm^{-1}, easily indicated by the rotational structure.

At higher wavenumbers, we observe the appearance of strong bands at 2845 (indicated by "A") and 2950 cm^{-1}, also corresponding to the modes of vibration for surface formates (C−H stretching of bidentate and bridged, respectively) reported elsewhere.[6,7,10] The band at 3660 cm^{-1} decreased after CO addition, consistent with reaction of CO with the geminal OH groups.

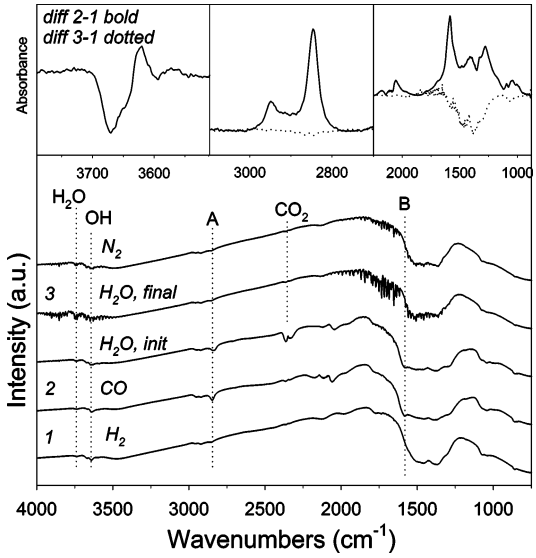

Figure 5. In-situ DRIFTS spectra starting from the bottom and moving upward: after re-reduction in H_2/N_2 and purging in N_2; after adsorption of CO and purging in N_2; after introducing H_2O/N_2 mixture; same spectra after 20 min; and finally after purging the H_2O using N_2. At the top, difference spectra are shown.

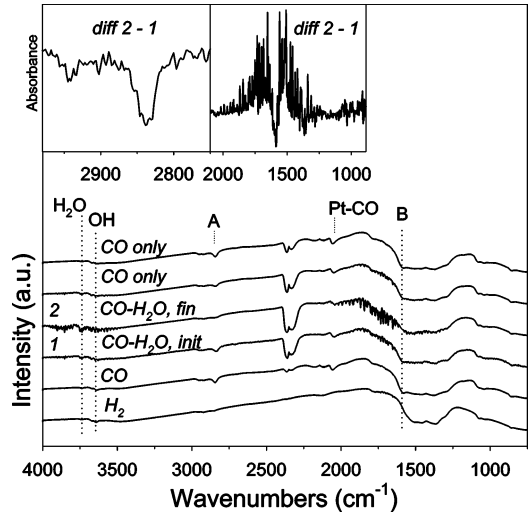

Figure 6. In-situ DRIFTS spectra starting from the bottom and moving upward: after re-reduction in H_2/N_2 and purging in N_2; after adsorption of CO; after initially introducing H_2O; and the same spectra after 30 min; and finally after removing the H_2O. At the top, difference spectra are shown.

In the second study, CO was again added at 350 °C, and the same bands were formed as before. However, after CO addition, the gas-phase CO was purged out with N_2 (135 cm^3/min), followed by addition of steam (125 cm^3/min) in N_2 (10 cm^3/min). Addition of the H_2O caused CO_2 to be liberated for several minutes, and during this time, the bands likely corresponding to formates (indicated by "A" and "B") and carbonates disappeared completely, as well as the band corresponding to Pt−CO (Figure 5). After addition of CO, there was again a decrease in the Ce−$(OH)_2$ geminal OH band at 3660 cm^{-1}.

In the third study, following H_2/N_2 addition, CO (3.75 cm^3/min) was added with N_2 (135 cm^3/min) a third time at 350 °C, and spectra were recorded (Figure 6). Then H_2O (125 cm^3/min) was introduced with the CO (3.75 cm^3/min) and N_2 (10 cm^3/min), and the reactants, surface species, and product CO_2 of the WGS reaction were observed as the concentrations reached steady state. Even with the presence of the numerous bands

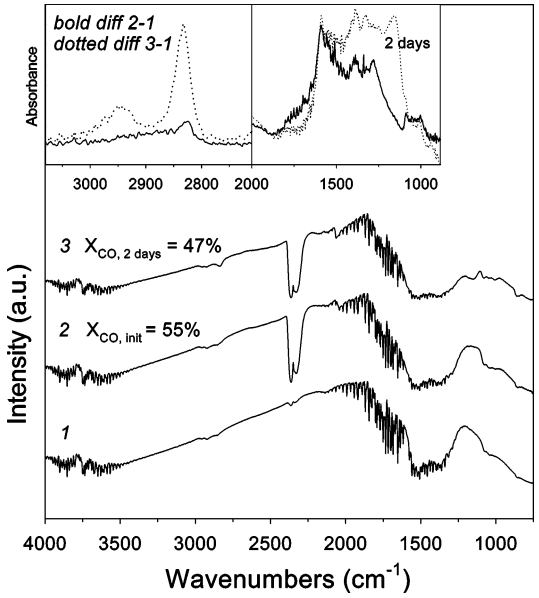

Figure 7. In-situ DRIFTS spectra starting from the bottom and moving upward: after re-reduction in H_2/N_2 and adsorption of H_2O; after initially introducing CO at 30 min time-on-stream for WGS; and after 2 days of catalyst deactivation. At the top, difference spectra are shown.

after water addition, the difference spectra depicted in Figure 6 indicate that H_2O addition removes the bands indicated by "A" and "B" under WGS reaction, as negative bands in the difference spectra appear at 2945, 2845, 1580, and 1370 cm^{-1}, consistent with the assignment of surface formates.[10]

The reverse procedure was conducted, whereby water was added first at 350 °C, followed by CO addition, as displayed in Figure 7. A small amount of surface formate is observed after taking the difference spectra at an initial CO conversion of 55%. After 2 days of deactivation, the CO conversion decreased to 47%, and the formate increased somewhat, as shown in the difference spectra. Interestingly, a band developed slowly over time at 1180 cm^{-1} with the deactivation of the catalyst. The identity of the band is currently not known, but may correspond to a carbonate species. Holmgren et al.[10] have noted assignments for bridged carbonate at 1130 and 1220 cm^{-1}, as well as an assignment at 1730 cm^{-1}. Certainly, the emergence of a band at approximately 1725 cm^{-1} is consistent with this assignment.

There is much discrepancy in the literature as to the assignments of bands for formate and carbonate species. Shido and Iwasawa[6,7] made assignments of bidentate formate at 2860, 1555, and 1360 cm^{-1}, while bidentate carbonate was assigned at 1575, 1290, and 1032 cm^{-1}, and unidentate carbonate was assigned at 1460, 1390, and 1060 cm^{-1}, respectively. Somewhat different assignments, as indicated previously, are given by Holmgren et al.[10] The band at 1560 is assigned to bidentate carbonate, while the band at 1580 cm^{-1} is assigned to formate. Hilaire et al.[5] concluded, on the basis of a comparison of the spectra in the region between 600 and 2200 cm^{-1} with spectra of $CaCO_3$, $SrCO_3$, and Na_2CO_3, that the bands formed were carbonates. However, no mention was made as to whether the higher wavenumber bands assigned to surface formates were observed in their study, as the range shown in their work includes only the region from 600 to 2200 cm^{-1}.

Therefore, before drawing further conclusions, we decided to try to obtain a better idea as to the nature of the bands, indicated by "A" and "B". First, it was important to determine how the bands responded in relation to each other. Therefore, the temperature was lowered in 10 °C increments from 350 °C to 200 °C, and the response of the bands to the decrease in

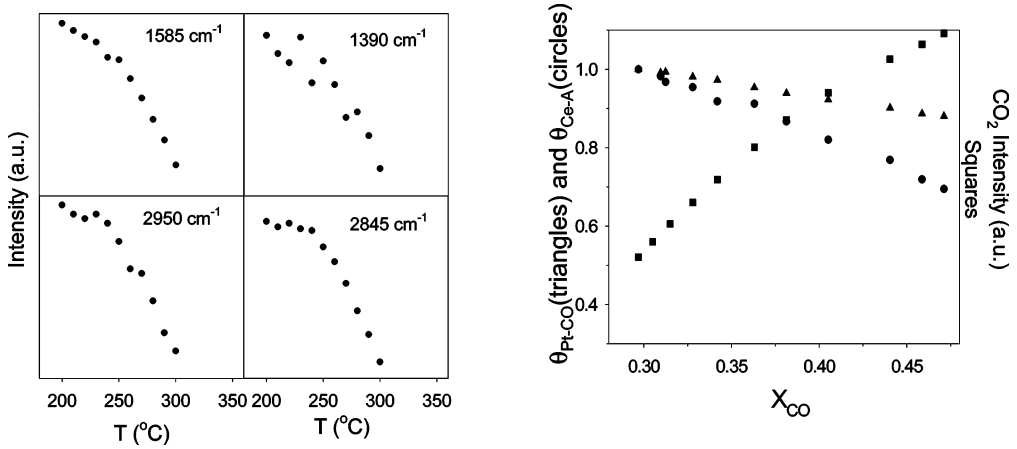

Figure 8. (Left) Response of IR bands at 1390, 1585, 2950, and 2845 cm^{-1} to temperature. (Right) Coverage of ceria by species A (C−H stretch of formate), coverage of Pt surface by CO, and CO_2 product intensity as a function of X_{CO}.

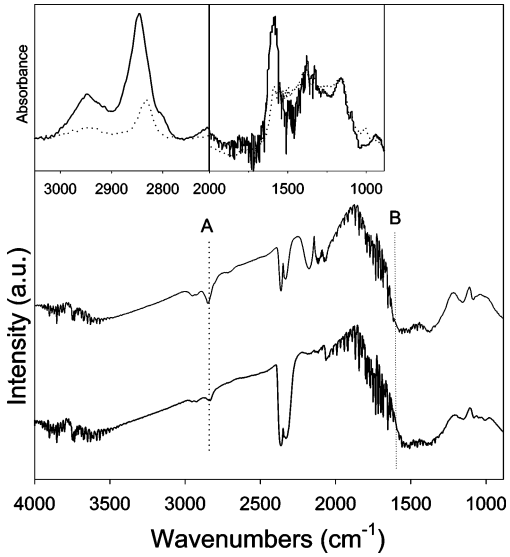

Figure 9. In-situ DRIFTS spectra under WGS at 350 °C (below) and 200 °C (above). At the top, difference spectra are shown, indicating the sharp increase in the surface concentration of species A (C−H stretch of surface formate) and species B (OCO asymmetric stretch of surface formate). Difference spectra are relative to the reduced catalyst, purged in nitrogen.

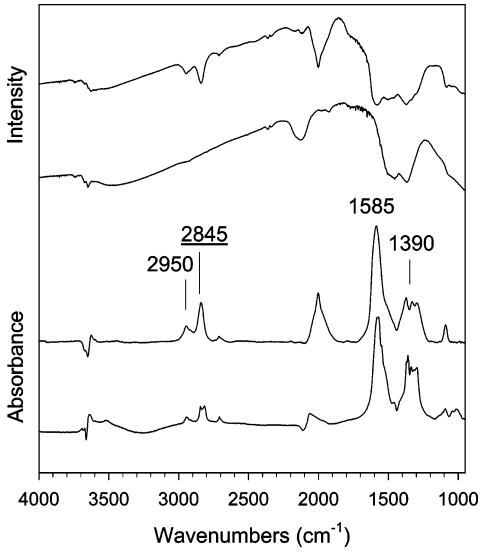

Figure 10. In-situ DRIFTS spectra of the adsorption of formic acid to 1% Pt/ceria (high-surface-area) at 350 °C for use as reference.

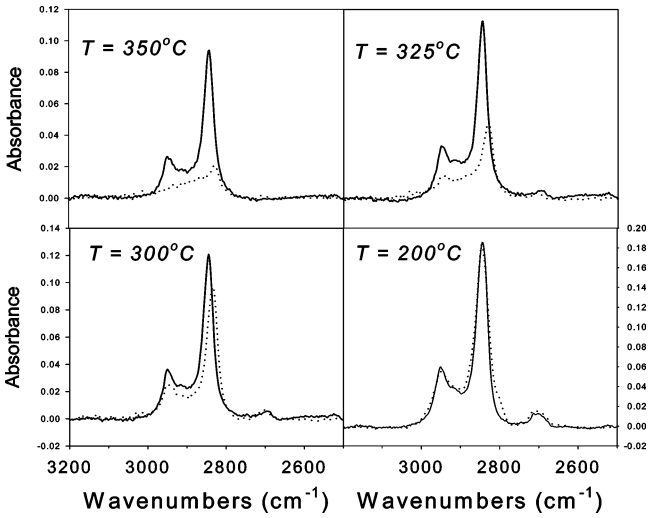

Figure 11. In-situ DRIFTS spectra of the adsorption of CO (bold) in inert N_2 carrier and after replacing the N_2 with H_2O under steady-state WGS reaction.

temperature, and therefore, CO conversion (X_{CO}), was monitored. As shown in Figure 8, the bands at 1390, 1585, 2950, and 2845 cm^{-1} very closely responded in a concerted manner, indicating that they are most likely the same species. Taking the low-temperature (200 °C) case, where the species reaches close to total coverage (as indicated by the leveling off of the peak intensities) as the total site density, coverages were calculated for the higher temperatures and plotted versus the CO conversion. While the CO almost entirely covers the surface of Pt throughout the range of temperatures, as also indicated by Hilaire et al.,[5] the coverage of species "A" and "B" largely diverge from the total site density with increasing reaction temperature (Figure 9).

To further clarify the confusion in the band assignments for this species, an additional experiment was conducted. Several 10 μL injections of formic acid were made into the N_2 carrier on the Pt/ceria high-surface-area catalyst (105 m^2/g) with the sample at 350 °C. As shown in Figure 10, the adsorption of formic acid resulted in the appearance of bands at 2845, 2950, 1585, and 1390 cm^{-1}, precisely the same band positions that characterize the identity of the strong bands A and B which emerge after CO adsorption. That is, "A" positioned at 2845 cm^{-1} corresponds to C−H stretching of bidentate formate, while "B" at 1585 cm^{-1} is the asymmetric OCO stretch vibration of the bidentate formate. The weaker C−H band at 2950 cm^{-1} is

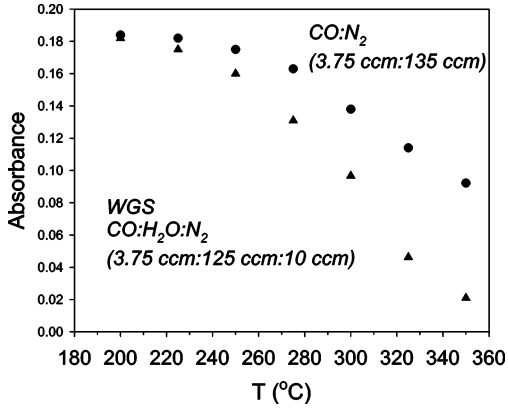

Figure 12. Intensities of formate species at 2845 cm^{-1} obtained from in-situ DRIFTS spectra of the adsorption of CO (circles) in inert N_2 carrier and after replacing the N_2 with H_2O under steady-state WGS reaction triangles over a wide range of temperatures.

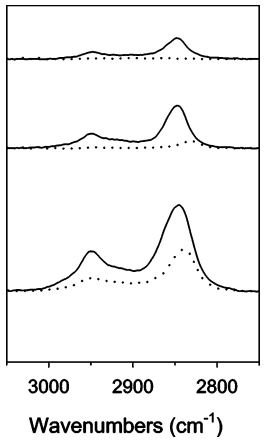

Figure 13. Formates were also rate limited for 1% Pt/ceria (high-surface-area). In-situ DRIFTS spectra of the adsorption of CO (bold) in inert N_2 carrier and after replacing the N_2 with water (dotted) under steady-state WGS reaction at, moving upward, 250 °C, 300 °C, and 350 °C.

likely a bridged formate, while the weaker 1390 cm^{-1} band is the formate OCO symmetric stretch vibrational mode. Our findings strongly suggest that surface formates are intermediates involved in the WGS mechanism, as concluded by Shido and Iwasawa.[6,7]

However, it was important to determine whether the sharp decline in surface formate concentration with increasing temperature (and therefore, WGS rate) was due to the reaction rate limiting the coverage, or whether it was due to the new concentration established by the adsorption/desorption equilibrium of CO.

Therefore, another experiment was made whereby the intensities of the high wavenumber formate band were monitored with CO addition in an inert N_2 flow and by replacing the N_2 with water at various temperatures to maintain constant CO partial pressure. Figures 11 and 12 indicate that at low temperatures (and low CO conversion), the formate is close to saturation on the surface of the ceria. However, at higher temperatures using a high H_2O/CO ratio where the CO dependency is first-order, the surface coverage of formate largely deviates from the equilibrium adsorption/desorption concentration. The important point is that the WGS reaction limits the surface concentration of surface formates,[13] while not affecting the Pt−CO coverage. Similar findings were obtained for the high-surface-area Pt/ceria catalyst, as shown in Figure 13. In the work of Hilaire et al.,[5] it was pointed out that O_2 addition was able to remove all bands in the OCO stretching (i.e., "carbonate") region. However, it is clear from this work that H_2O addition only significantly influences the bands specifically correlating to those of the formates (i.e., 1585 and 1390 cm^{-1}), while the remaining bands in that region are affected very little, if at all. Figure 14 shows that at all temperatures studied in this work, whether the catalyst was under CO adsorption or WGS reaction, the CO coverage on Pt did not change significantly.

Therefore, these data suggest that A and B are vibrational modes corresponding to the same adsorbed surface formate species, and the surface formates are likely intermediates for the water-gas shift reaction (C−H and OCO stretching), consistent with the following observations.

·After adsorption of CO and purging in N_2, addition of H_2O generates CO_2 for several minutes, and band A decreases and disappears.

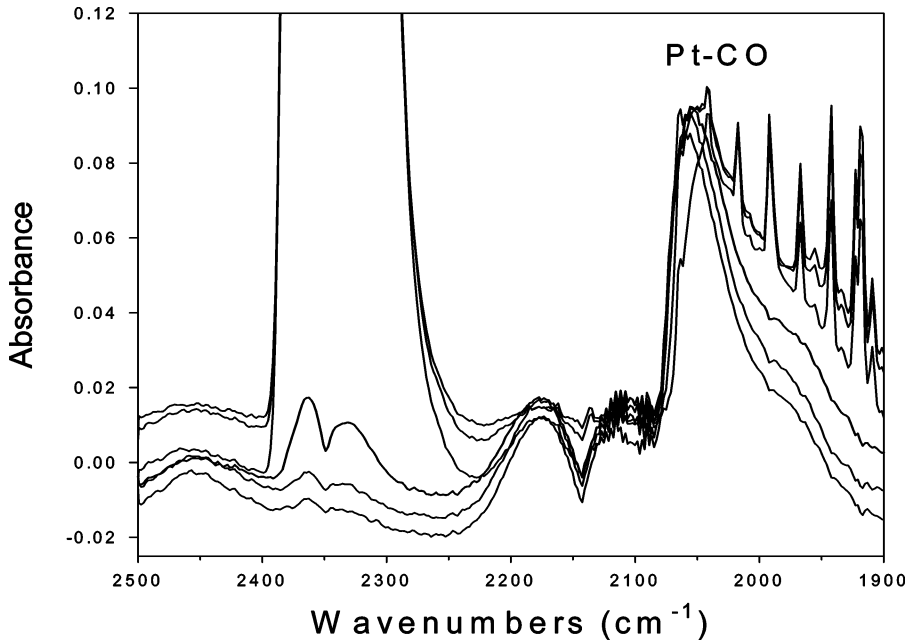

Figure 14. In-situ DRIFTS spectra of the adsorption of CO (bold) in inert N_2 carrier and after replacing the N_2 with H_2O under steady-state WGS reaction over a wide range of temperatures. Spectra indicate that the Pt−CO intensity changes very little under all conditions.

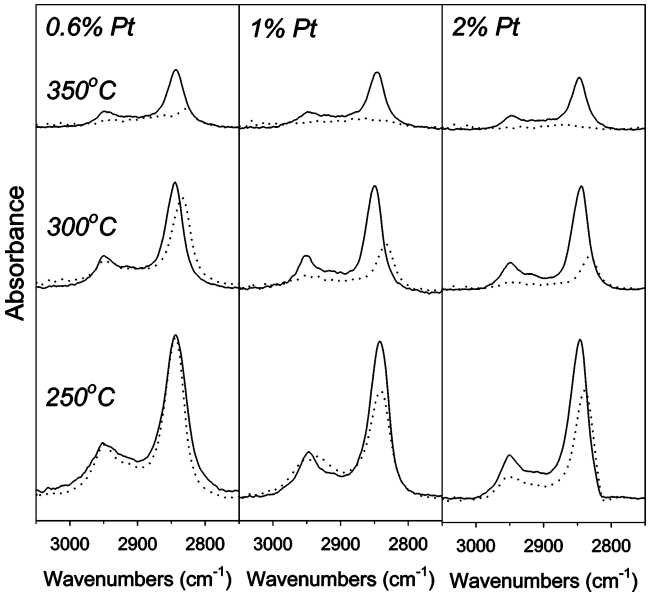

Figure 15. Steady-state concentrations of surface formate species as a function of loading and temperature. Solid lines indicate adsorption of CO in N_2, and the dotted lines display the catalyst under WGS reaction conditions, whereby the N_2 balancing gas was replaced by H_2O to maintain a constant CO partial pressure.

·After adsorption of CO in N_2, addition of H_2O with the CO by replacing N_2 generates CO_2 and band A decreases to a steady-state value.

·Deactivation of the catalyst results in an increase in band A on the catalyst surface.

·The coverages of surface formates decline sharply with increasing reaction temperature and, therefore, CO conversion.

·The coverages of surface formates are limited by the WGS reaction, but are close to the equilibrium adsorption/desorption surface concentrations at low conversion.

However, it is difficult to eliminate either the bidentate formate[6,7] or ceria redox process[4,5,9] on the basis of the current study. More conclusive kinetic evidence is required by testing catalysts under a wide range of conditions. Also, future in-situ XANES testing would be helpful for developing a better understanding of the oxidation-state changes of ceria that occur under different reaction environments in order to find direct evidence to substantiate the ceria-mediated redox process. The utility of the XANES technique for CeO_2 catalysts has already been demonstrated for automobile catalytic convertor catalysts (ACCC).[14,15] Certainly oxygen transfer from ceria does play an important role in oxidation during excursions of the air/fuel ratio into the fuel-rich regime.[16]

From the standpoint of activity, either mechanism requires the close interaction of noble metal with the support. For the ceria-mediated redox process, the interface between noble metal and ceria is required, whereas for the bidentate formate mechanism, reduction of the ceria surface with the help of the noble metal allows for the formation of geminal OH groups (proposed active sites) on the partially reduced ceria surface. Therefore, decreasing domain size of ceria (using nanostructured materials) and improving dispersions and loadings of noble metal will likely lead to more highly active catalysts. Surface formates were found to be more rate limited at higher loadings, as evidenced in Figure 15.

At higher surface areas obtained by the use of nanostructuring methods, catalysts will likely need stabilization by other materials in order to prevent growth of ceria domains, and perhaps as well to prevent buildup of carbonates. The detrimental effect of carbonates was suggested previously by Hilaire et al.,[5] but more definitive studies are required.

4. Conclusions

Steady-state IR measurements continue to favor the bidentate formate mechanism explaining WGS. However, more kinetic studies are required over a wide range of temperatures. While low-temperature kinetic studies have found a zero-order dependency for CO and relate this to saturation of noble metal surface, this study indicates that CO is also close to saturation at low temperature as an adsorbed formate on the partially reduced ceria. In this work, a high H_2O/CO ratio was employed, where the CO dependency is first-order. This implies the adsorbed CO intermediate should move to sparser coverages with the rate. At low temperatures, where CO conversion was low, both Pt−CO and formates were close to their equilibrium adsorption−desorption values. Inert balancing gas was replaced by water in these studies to keep the same partial pressure of CO. At higher temperatures, however, where CO conversion was high, the surface formates were found to be substantially limited by the WGS reaction, while Pt−CO remained relatively unchanged.

References and Notes

(1) Fuel Cell Handbook, 5th ed.; US DOE, NETL, 2000.
(2) Dayton, D. C.; Ratcliff, M.; Bain, R. Fuel Cell Integration−A Study of the Impact of Gas Quality and Impurities, NREL/MP-510-30298, 2001.
(3) Ghenciu, A. F. Curr. Opin. Solid State Mater. Sci. **2002**, *6*, 389.
(4) Bunluesin, T.; Gorte, R. J.; Graham, G. W. *Appl. Catal. B* **1998**, *15*, 107.
(5) Hilaire, S.; Wang, X.; Luo, T.; Gorte, R. J.; Wagner, J. *Appl. Catal. A* **2001**, *215*, 271.
(6) Shido, T.; Iwasawa, Y. *J. Catal.* **1993**, *141*, 71.
(7) Shido, T.; Asakura, K.; Iwasawa, Y. *J. Catal.* **1990**, *122*, 55.
(8) Lavalley, J. C. *Catal. Today* **1996**, *27*, 377.
(9) Li, Y.; Fu, Q.; Flytzani-Stephanopoulos, M. *Appl. Catal. B* **2000**, *27*, 179.
(10) Holmgren, A.; Andersson, B.; Duprez, D. *Appl. Catal. B* **1999**, *22*, 215.
(11) Yao, H. C.; Yao, Y. F. Y. *J. Catal.* **1984**, *86*, 254.
(12) Jacobs, G.; Williams, L.; Graham, U.; Thomas, G. A.; Sparks, D. E.; Davis, B. H. *Appl. Catal. A, Gen.*, in press.
(13) Jacobs, G.; Graham, U.; Davis, B. H. Tri-State Catal. Spring Symp. (May, 2002).
(14) Overbury, S.; Huntley, D.; Mullins, D.; Glavee, G. *Catal. Lett.* **1998**, *51*, 133.
(15) El Fallah, J.; Boujana, S.; Dexpert, H.; Kiennemann, A.; Majerus, J.; Touret, O.; Villain, F.; Le Normand, F. *J. Phys. Chem.* **1994**, *98*, 5522.
(16) Hertz, R.; Sell, J. *J. Catal.* **1985**, *94*, 166.